Electronic Supplementary Information (ESI)

The Promotion Effect of Isolated Potassium Atoms with Hybridized Orbitals in Catalytic Oxidation

Fei Xu, Zhiwei Huang, Pingping Hu, Yaxin Chen, Lei Zheng, Jiayi Gao, Xingfu Tang*

Contents:

1. Experimental Section

1.1. Catalyst syntheses and alkali loadings

The HMO was prepared by a hydrothermal route with an aqueous solution of manganese sulfate monohydrate ($MnSO_4 \cdot H_2O$, 0.20 mol L^{-1}), ammonium persulfate ($(NH_4)_2S_2O_8$, 0.20 mol L^{-1}) and ammonium sulfate ($(NH_4)_2SO_4$, 1.00 mol L^{-1}) at 120 ^oC for 12 hours. The obtained black solid was dried at 110 ^oC for 24 hours and calcined at 400 ^oC for 4 hours. Potassium was loaded by impregnating the HMO powder with an aqueous solution of KCl, and the concentration of the KCl solution was adjusted to obtain the different potassium loadings, followed by being dried at 110 ^oC for 12 hours to give KCl/HMO. K_1/HMO with different K^+ loadings were obtained after annealing the KCl/HMO at 400 ^oC for 12 hours and then washing the sample by deionized H_2O (3000 mL) at room temperature.[1] The Potassium loadings were determined by using X-ray Fluorescence Spectrometer (XRF) on a Bruker-AXS S4 Explorer.

1.2. STEM, EDX, TEM and HRTEM images

Transmission electron microscopy (TEM), high resolution TEM (HRTEM) images were obtained on a JEM 2100F transmission electron microscope. High-angle annular dark field scanning transmission electron microscopy (HAADF-STEM) and line-scanned energy dispersive X-ray (EDX) spectra were obtained on a Titan S/TEM (FEI) transmission electron microscope. The HAADF-STEM image simulations were conducted using the QSTEM software using the multislice algorithm.[2] In the simulations, spherical aberration coefficient of 0.5 mm, defocus -43.4 nm and Scherzer focus were used.

1.3. X-ray diffraction patterns and Rietveld refinements

The synchrotron X-ray diffraction (SXRD) patterns were performed at beamline 14B of the Shanghai Synchrotron Radiation Facility at a wavelength of 0.6887 Å. A Mar345 image plate detector

was employed for the data collection and the data were further integrated using the fit2d code.[3] The beam is mono-chromatized using Si(111) and a Rh/Si mirror was used for the beam focusing to a size of around 0.5 mm × 0.5 mm. Rietveld refinements of the diffraction data were performed with the FULLPROF software package on the basis of the space group *I*4/*m*.

1.4. X-ray absorption spectra

The X-ray absorption spectra (XAS) of the samples including the X-ray absorption near-edge structure (XANES) spectra and extended X-ray absorption fine structure (EXAFS) spectra at the K *K*-edge were measured at beamline 4B7A of the Beijing Synchrotron Radiation Facility with electrons beam energy of 2.21 GeV and a ring current of 300-450 mA. The XAS data were collected with a fixed exit monochromator using two flat Si(111) crystals. The XANES spectra were recorded with an energy step of 0.5 eV. The EXAFS spectrum of the reference sample (here KCl) was collected in a transmission mode using low-pressure ion chambers filled with Kr, while partial fluorescence yield mode was adopted for the K_1/HMO samples using a silicon drifted detector (e2v, UK). The raw data was analysed using the IFEFFIT 1.2.11 software package.[4]

1.5. X-ray photoelectron spectra

The X-ray photoelectron spectra (XPS) analysis was undertaken using Kratos Axis Ultra-DLD system with a charge neutralizer and a 150 W Al (Mono) X-ray gun (1486.6 eV). The spectrometer was equipped with a delay-line detector (DLD). Spectra were acquired at normal emission with a passing energy of 40 eV. The XPS were referenced to the C 1*s* peak at the binding energy of 284.6 eV. Data analysis and processing were undertaken using XPSPeak 4.1 with the Shirley type background.

1.6. NO-TPD analyses

The NO temperature-programmed desorption (NO-TPD) procedure was conducted after the saturated adsorption of NO was finished at 250 °C. The catalyst (500 mg) after adsorption saturation of NO was purged by pure N_2 to remove physically adsorbed NO species on the surface, and subsequently heated from 250 to 400 °C at a ramp of 10 °C min^{-1} in a flow containing 3.0 vol.% O_2 balanced by N_2 (500 mL min^{-1}). The concentrations of NO and NO_2 in the outlet gases were measured by an online chemiluminescence NO-NO_2-NO_x analyzer (42*i*-HL, High Level, Thermo Electron Corporation). The desorption amount was calculated according to the integral area of the corresponding desorption curve.

1.7. Calculation of the number of adsorbed NO molecules from NO-TPD

The number of adsorbed NO molecules of the HMO and the K_1/HMO by NO-TPD was calculated as follows:

(i) *Average density of the unit cell of the HMO and the K_1/HMO.*

The mass (M_{cell}) of one unit cell is calculated based on the formula of the HMO and the K_1/HMO (Table S1). The volume (V_{cell}) of one unit cell according to the lattice parameters (*a* and *c*) obtained from the Rietveld refinements and the tetragonal structure feature of the HMO and the K_1/HMO can be calculated as follows:

$$V_{cell} = a^2 \times c.$$

Thus, the average density (ρ) of the unit cell of the HMO and the K_1/HMO is given:

$$\rho = M_{cell} / V_{cell} = M_{cell} / (a^2 \times c).$$

(ii) *The number of the nanorods for 500 mg catalyst*.

The volume (V_{rod}) and mass (M_{rod}) of single HMO or K_1/HMO nanorod are calculated according to the length and width distributions from the TEM and HRTEM images:[5]

$$V_{rod} = w^2 \times l,$$

$$M_{rod} = V_{rod} \times \rho = w^2 \times l \times M_{cell} / (a^2 \times c),$$

where w and l represent the average width (w =13 nm) and length (l = 470 nm) of the HMO or the K_1/HMO nanorods. Therefore, the number (N_{rod}) of the HMO or the K_1/HMO nanorods (M_{cat} = 500 mg) is calculated as follows:

$$N_{rod} = M_{cat} / M_{rod} = M_{cat} \times a^2 \times c / (w^2 \times l \times M_{cell}).$$

(iii) *The number of the tunnel openings of 500 mg catalyst*.

The number of the tunnel openings on the {001} top-facets ($N_{opening}$) of the HMO and the K_1/HMO nanorods can be calculated:

$$N_{opening} = (w^2 / a^2 \times 2 \times 2) \times N_{rod} = (w^2 / a^2 \times 2 \times 2) \times M_{cat} \times a^2 \times c / (w^2 \times l \times M_{cell}) = 4 \times M_{cat} \times c / (l \times M_{cell}),$$

where the expression in the parentheses is used to calculate the number of the tunnel openings of single HMO or K_1/HMO nanorod, the first number "2" represents two ends of single HMO or K_1/HMO nanorod, and the second "2" does two tunnel openings in each unit cell of the HMO or the K_1/HMO.

(iv) *The number of the adsorbed NO molecules by NO-TPD*.

The total adsorption number (Q) of NO molecules was calculated according to the integral area of the corresponding desorption curves. Therefore, the number (N_{NO}) of adsorbed NO molecules per opening of the HMO or the K_1/HMO can be obtained:

$$N_{NO} = Q / N_{opening}.$$

1.8. Catalytic evaluations

1.8.1 Catalytic oxidation of HCHO

The oxidation of HCHO was performed in a fixed-bed quartz reactor (i.d. = 8 mm) under atmospheric pressure. The catalyst (50 mg, 40-60 mesh) was loaded for each run. Gaseous formaldehyde (HCHO) was generated by passing a N_2 gas flow over paraformaldehyde (96%, Acros) in an incubator kept at 45 ^oC, and then mixed with an O_2 flow, leading to a feed gas containing 150 ppm HCHO and

10.0 vol.% O_2 balanced by N_2. The total flow rate was 100 mL·min^{-1}. The effluents from the reactor were analyzed with an on-line Agilent 7890A gas chromatograph equipped with TCD and FID detectors. In order to compare the pre-exponential factors (F_p), Arrhenius plots of reaction were drawn. The surface reaction kinetics of the HCHO oxidation was conducted at low temperature over the K_1/HMO and the potassium-free HMO at the conversions of HCHO less than 20% to achieve the data of the intrinsic reaction kinetics. The HCHO concentration ranged from 140 to 560 ppm, and the corresponding O_2 concentration ranged from 700 to 2100 ppm. The data were recorded up to the steady state for each run.

1.8.2 Catalytic oxidation of ethyl acetate

The complete oxidation of ethyl acetate was performed in a fixed-bed quartz reactor (i.d. = 8 mm) under atmospheric pressure. The catalyst (50 mg, 40-60 mesh) was loaded for each run. Gaseous ethyl acetate was generated by passing a N_2 gas flow over ethyl acetate (99.5%, Shanghai Chemical reagent Co., LtD) in an incubator kept at 0 ^{o}C, and then mixed with an air flow, leading to a feed gas containing 800 ppm ethyl acetate and 20.0 vol.% O_2. The total flow rate was 200 mL min^{-1}. The effluents from the reactor were analyzed with an on-line Agilent 7890A gas chromatograph equipped with TCD and FID detectors. The data were recorded up to the steady state for each run.

1.9. Calculation of the TOF

The catalytic activity in terms of a turnover frequency (*TOF*, the number of converted HCHO molecules per catalytically active site and per second) is calculated as follows:

The number of converted HCHO molecules (N_{conv}) per one second for 50 mg catalyst can be calculated according to the number of the fed HCHO molecules (N_{HCHO}) per one second and the conversion rate of HCHO (η) at set reaction temperature.

$N_{conv} = N_{HCHO} \times \eta = (N_A \times C_0 \times V_s / V_m) \times \eta = 6.02 \times 10^{23}$ mol^{-1} $\times$ $1.50 \times 10^{-4} \times 1.67 \times 10^{-3}$ L $\div$ (22.4 L·mol^{-1}) $\times$ $\eta = 6.73 \times 10^{15} \times \eta$,

where N_A is the Avogadro constant (6.02×10^{23} mol^{-1}), C_0 is the concentration in volume fraction of the fed HCHO (1.50×10^{-4}), V_s is the volume of the fed total gases that pass the catalyst in one second (100 mL min^{-1} $\times$ (1 min / 60 s) $\times$ 1 s = 1.67×10^{-3} L), and V_m is the standard molar volume of gas (V_m = 22.4 L mol^{-1}).

Then, the *TOF* during the time (t) of one second can be calculated as:

$TOF = (N_{conv} / N_{opening}) / t = \{6.73 \times 10^{15} \times \eta \div [4 \times M_{cat} \times c / (l \times M_{cell})]\} \div 1$ s.

Therefore, the *TOF* at different reaction temperatures were calculated according to the conversion of HCHO at the corresponding temperatures in Fig. S5. The values of $N_{opening}$, M_{cat} and M_{cell} have been defined and calculated in the section 1.7 above.

2. Tables and Figures

Table S1. Crystallographic data and details of the HMO and the K_1/HMO with the K occupancy factor[6] of 0.5 in the SXRD data collections and the Rietveld refinements.

Samples	HMO	K_1/HMO
Chemical formula	MnO_2	$K_{0.125}MnO_2$
Crystal system	tetragonal	tetragonal
Space group	*I*4/*m*	*I*4/*m*
Z [a]	8	8
a / Å	9.844(5)	9.887(0)
c / Å	2.867(6)	2.871(5)
V / Å^3	277.9(1)	280.6(9)
R_p [b] / %	1.81	1.67
R_{wp} [c] / %	2.64	2.59
R_{exp} [d] / %	1.86	1.81
χ^2 [e]	2.01	2.04
Wavelength / Å	0.6887	0.6887
2θ range / °	3-80	3-80
2θ step width / °	0.02	0.02

[a] Z, the number of MnO_2 and $K_{0.13}MnO_2$ formula units per unit cell;

[b] R_p, the unweighted profile factor;

[c] R_{wp}, the weighted profile factor;

[d] R_{exp}, the expected R parameter;

[e] χ^2, the goodness of fitting, defined as the square of the ratio of R_{wp}/R_{exp}.

Table S2. Structure parameters of the HMO and the K_1/HMO with the K occupancy factor[6] determined by the Rietveld refinement of the corresponding SXRD data.

Samples	Atom	*x*	*y*	*z*	Occupancy factor[a]
HMO	Mn	0.3525(6)	0.1692(3)	0	1.0
	Oi	0.1451(5)	0.2024(8)	0	1.0
	Oii	0.5326(4)	0.1682(7)	0	1.0
K_1/HMO	K	0	0	0.5	0.5
	Mn	0.3499(1)	0.1680(9)	0	1.0
	Oi	0.1549(3)	0.1989(7)	0	1.0
	Oii	0.5450(1)	0.1671(9)	0	1.0

[a]Occupancy factor × Wyckoffnumber = number of atoms/unit cell.

Table S3. EXAFS parameters at the K *K*-edge of the K_1/HMO and KCl with the k^2 weight.[a]

Samples	Shell	*CN* [b]	*R* [c] / Å	σ^2 [d] / Å^2	ΔE_0 [e] / eV
K_1/HMO	K-Oi	8	2.89(4)	0.005(6)	+ 2.6
	K-Oii	4	3.35(2)	0.013(2)	- 1.5
	K-Mn	4	3.59(1)	0.016(3)	+ 6.4
KCl	K-Cl	6	3.14(8)	0.010(8)	+ 3.9
	K-K	12	4.48(0)	0.017(8)	- 4.4

[a] *R*-space fit, Δk = 1.7-8.2 Å^{-1}, Δr = 1.0-5.0 Å;

[b] *CN*, coordination number;

[c] *R*, distance between absorber and backscatter atoms;

[d] σ^2, Debye-Waller factor;

[e] ΔE_0, energy shift.

Table S4. Atom distances of K_1/HMO determined by the Rietveld refinement of the corresponding SXRD data.

Shell	*CN* [a]	Distance / Å
K-O_i	8	2.87(6)
K- O_{ii}	4	3.31(1)
K-Mn_i	4	3.60(2)
K-Mn_{ii}	4	4.09(7)

[a] *CN*, coordination number.

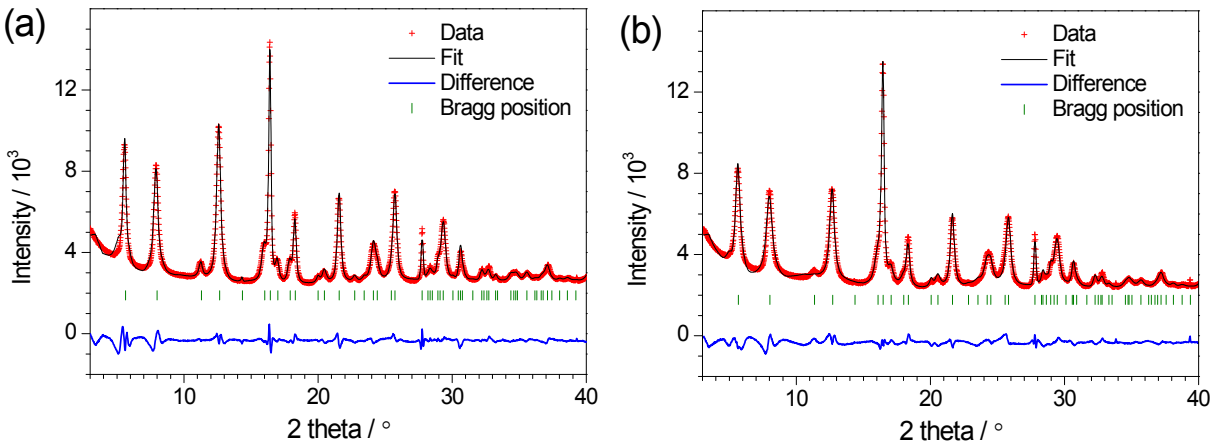

Fig. S1 SXRD patterns of the K_1/HMO (a) and the HMO (b) including the Rietveld refinement.

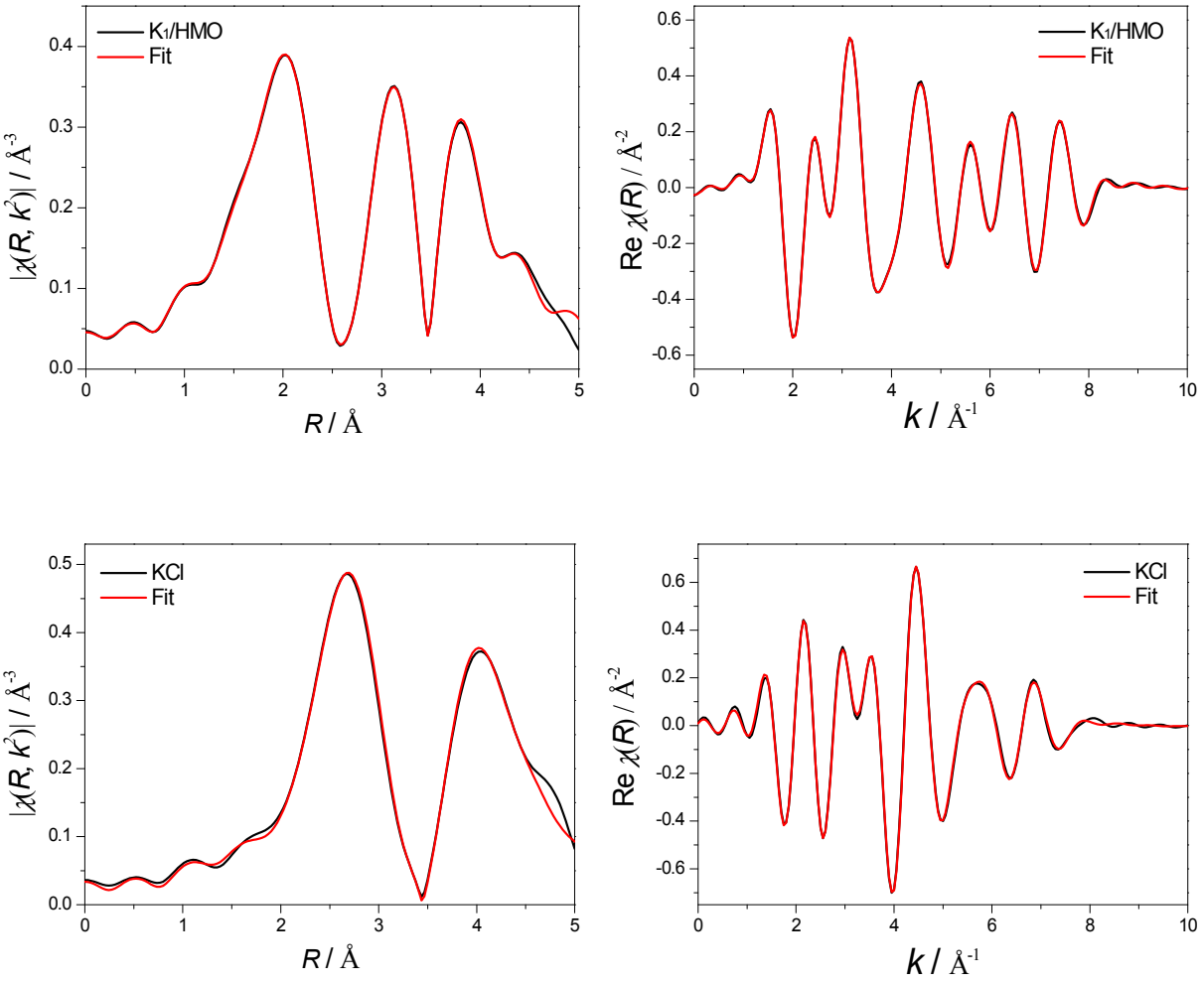

Fig. S2 *R*-space (Δk = 1.7-8.2 Å^{-1}) and inverse FT spectra (Δr = 1.0-5.0 Å) at the K *K*-edge of the K_1/HMO and KCl with the k^2 weight.

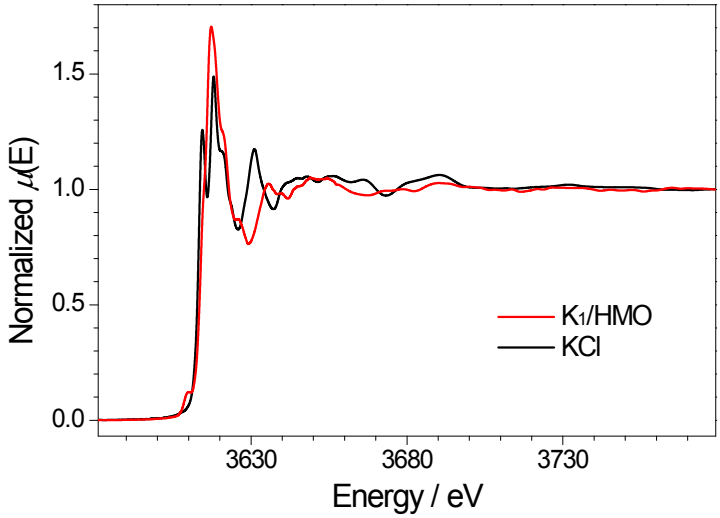

Fig. S3 XANES spectra at the K *K*-edge of the K_1/HMO and KCl.

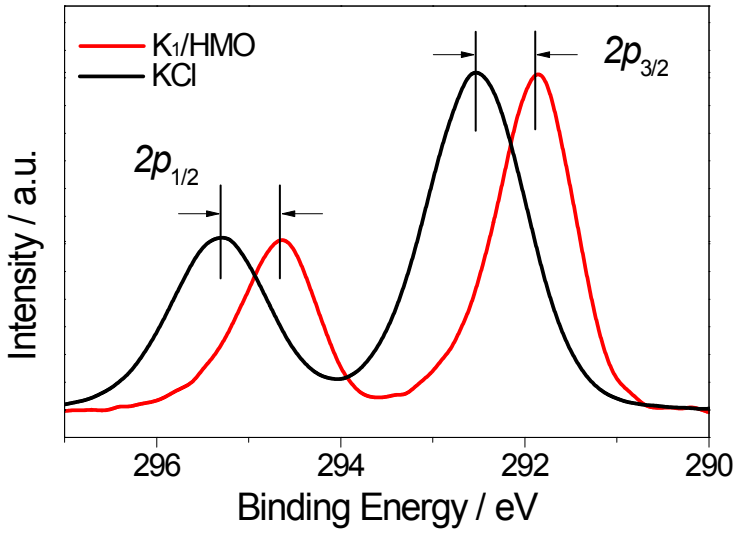

Fig. S4 K 2*p* XPS of K_1/HMO and KCl showing the shift of binding energy.

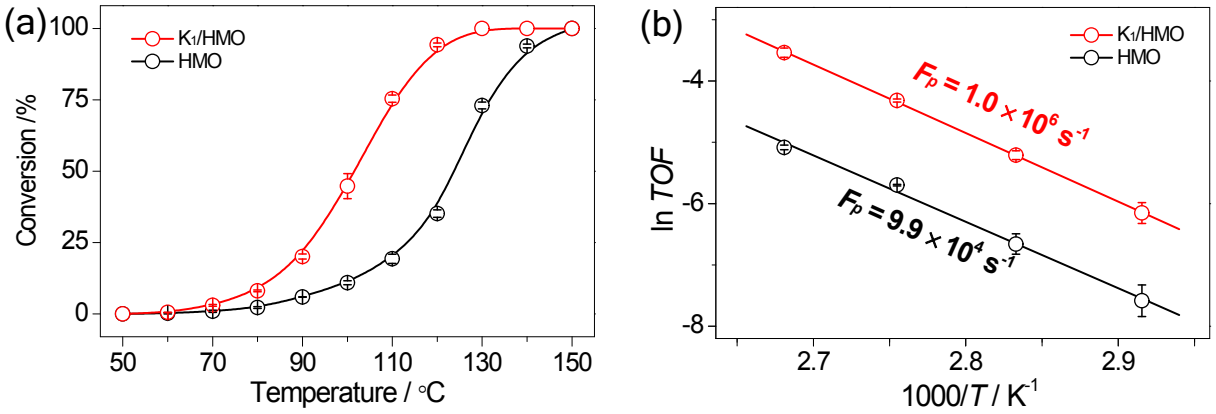

Fig. S5 (a) The conversion of HCHO over K_1/HMO and the potassium-free HMO as a function of reaction temperature. (b) Arrhenius plot for the *TOF* with the pre-exponential factors (F_p) of HCHO oxidation over the K_1/HMO and the HMO.

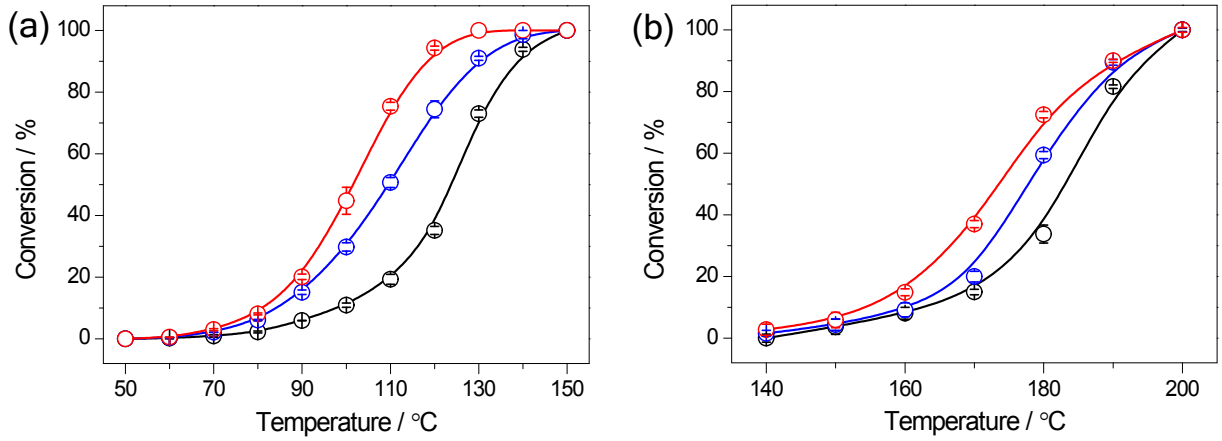

Fig. S6 HCHO conversion (a) and ethyl acetate conversion (b) over K_1/HMO and HMO as a function of the reaction temperature. The black line represents HMO, and the red and blue lines represent the K_1/HMO with the K occupancy factors[6] of 0.50 and 0.25, respectively.

3. References

1 Z. Huang, X. Gu, W. Wen, P. Hu, M. Makkee, H. Lin, F. Kapteijn and X. Tang, *Angew. Chem. Int. Ed.*, 2013, **52**, 660-664.

2 C. Koch, *PhD Thesis* (Arizona State University), 2002.

3 J. Y. Kim, J. A. Rodriguez, J. C. Hanson, A. I. Frenkel and P. L. Lee, *J. Am. Chem. Soc.*, 2003, **125**, 10684-10692.

4 M. Newville, *J. Synchrotron Radiat.*, 2001, **8**, 322-324.

5 Z. Huang, X. Gu, W. Wen, P. Hu, M. Makkee, H. Lin, F. Kapteijn and X. Tang, *Angew. Chem., Int. Ed.*, 2013, **52**, 660-664.

6 J. Vicat, E. Fanchon, P. Strobel, D. T. Qui, *Acta Crystallogr. B*, 1986, **42**, 162-167.